STM JOURNALS

Research & Reviews:
Discrete Mathematical Structures

ISSN: 2394-1979
Volume 11, Issue 2, 2024
May–August
DOI Journal: 10.37591/RRDMS

https://journals.stmjournals.com/rrdms

Research RRDMS

Human Skin Abnormality Detection with Process Similarity Criteria Fit Machine Learning Method

Arkadiy Dantsker[1,*], Aleksandr Veksler[2]

Abstract

This method presents a machine learning method that satisfies the defined conditions for healthy waterside beach activities. The boundary conditions of the normal and abnormal radiation spaces were formulated. The objectives of using a Regression Polynomial with Process Similarity Criteria Fit for skin temperature prediction are justified by the analysis of the existing analytical and machine learning approaches. An algorithm for skin temperature prediction using the theories of similarity criteria fit and hypernumber is presented. A computational approach for identifying radiation abnormalities is provided. The proposed machine learning method for skin temperature prediction was compared with the minimum least-squares regression and long short-term memory (LSTM) neural network methods. The schema for monitoring skin temperature and implementing the prediction algorithm coverage includes a Raspberry PI Zero mini-computer and a sensor that satisfies accuracy and integration with Raspberry. The practical application of this approach is enabled by a monitoring system featuring a Raspberry Pi Zero mini-computer and compatible sensors. This configuration ensures precise data collection and smooth integration of the prediction algorithm, offering an affordable and efficient solution for real-time skin temperature monitoring. The proposed system was designed to improve beachgoer safety by delivering timely alerts and recommendations based on real-time data analysis.

Keywords: Similarity, criteria, regression, hypernumber, temperature

INTRODUCTION

The effects of solar radiation on the skin can be either beneficial or harmful [1]. Intelligent control of the irradiance duration protects against skin cancer and provides pain relief. In conclusion, extreme sun exposure leads to thermal burns, photocarcinogenesis (initiation of cancer), and photoaging due to tissue heating, rather than an isolated effect of infrared radiation (IR). The strong associations between sunburn and a variety of skin cancers, including melanoma are provided in the research paper [2]. Exposure to beaches and waterside activities has been linked to melanoma in multi-country European research studies [3].

According to Peterson et al. [4], the major factors that cause carcinogenesis are exposure to high temperatures and ultraviolet radiation (UVR). IR, as per the analysis in this study, is a secondary factor that increases the possibility of carcinogenesis. The ratio of IR-to-UVR radiation was approximately 49:7. However, UVR above normal levels is the main cause of sunburn, tissue injury, and DNA damage [5]. The human skin temperature can be increased to 40°C because of intense sunlight [6]. Early prediction of skin temperature abnormalities with high accuracy and efficiency can prevent the negative effects of solar radiation.

According to the conclusions presented in previous studies, the harmful effects of solar

*Author for Correspondence
Arkadiy Dantsker
E-mail: amdantsker@gmail.com

[1]Principal Investigator, Detex Analytics, LLC, Kirkland WA, USA
[2]Researcher, Detex Analytics, LLC, Kirkland WA, USA

Received Date: August 12, 2024
Accepted Date: August 27, 2024
Published Date: August 30, 2024

Citation: Arkadiy Dantsker, Aleksandr Veksler. Human Skin Abnormality Detection with Process Similarity Criteria Fit Machine Learning Method. Research & Reviews: Discrete Mathematical Structures. 2024; 11(2): 17–24p.

radiation are caused by a combination of tissue heating and radiation (IR and ultraviolet). These beneficial and harmful conditions can translate into both normal Ω_{norm} and abnormal Ω_{abnorm} physical spaces. The conditions for such spaces are formulated in Equations (1) and (2) as follows:

$$\Omega_{norm} = \{(t_{skin}, q_r): t_{skin} < t_{skin\_max} \cap q_r < q_{r.max} \forall (t_{skin}, q_r) \in \Omega_{norm}\}. \quad (1)$$

$$\Omega_{abnorm} = \{(t_{skin}, q_r): t_{skin} \geq t_{skin\_max} \cup q_r \geq q_{r.max} \ (t_{skin}, q_r) \in \Omega_{norm}\} \quad (2)$$

The current study aimed to define a model that prevents excessive sun exposure that corresponds to an abnormal space.

An analysis of the applicability of the existing model to reach the target is discussed below.

The development of thermal models for human skin temperature is important. These models include the internal heat generated by sun radiation penetration [7], heat exchange expression, and boundary conditions at the skin surface [8]. The accuracy of the models can be significantly improved by adaptive approaches [9–11] with analytical solutions based on the theory of hypernumbers [12, 13] and by solving the operator equations with hypernumbers theory [14]. Analytical thermal models of human skin protected by clothing under sunlight radiation have been defined by Lai et al. [15]. The model exhibited a low accuracy at extremely low temperatures. The difference between the monitored and predicted temperatures was up to 6F. Analytical thermal modeling of skin temperature can be used as an alternative or complementary method to machine learning algorithms.

Random forest, decision, vector machine, and K-neighborhood were trained to define the most accurate machine learning model for skin temperature prediction [16]. The model trained using the Random Forest showed the best accuracy of 90,4%. A deep learning algorithm with the skin sensitivity index SSI was proposed to overcome individual differences and variations in skin subtleness [17].

The disadvantages of the machine learning models used for skin prediction are as follows:

- High computational complexity [18].
- The most efficient machine learning models, such as neural networks (RNN), long short-term memory (LSTM) neural networks, and Random Forest models, provide numerical results. Such results require a highly complex algorithm to identify radiation abnormalities.
- The existing regression models have low accuracy in predicting and are not applicable for high-quality prognostics.

Analytical Method of the Skin Temperature Prediction

The prediction is provided using Regression Polynomials with Process Similarity Criteria [19] for stochastic data defined by hypernumber H_k. Using this method, the solution should satisfy the following expression:

$$L = min \sum_{i=0}^{n} (v_i - \bar{v})^2 \quad (3)$$

Where, $m = 2l, l \epsilon N \ (natural\ number)$ – is the sample size for calculating the variance at point i, $\bar{v}$ is the mean variance of the sample, and the v_i is the variance at state i that can be approximately calculated using the segmentation approach [20]:

$$v_i = \frac{\sum_{j=i-\frac{m}{2}}^{j=i+\frac{m}{2}} \left(T_j^{m.sk} - T_j^{t.sk}\right)^2}{m-1} \quad (4)$$

where $T_j^{m.sk}$ and $T_j^{t.sk}$ are monitored, and the theoretical temperature of the skin at moment j is

$$T_j^{t.sk} = a_0 + a_1 t_j + \cdots + a_n t_j^n \quad (5)$$

where $a_0, a_1, \ldots, a_n$ are the coefficients of the polynomials that satisfy the method criteria.

The coefficients of the polynomial are defined using the standard approach for determining the min. (max.) for the multivariable operator:

$$\begin{cases} \dfrac{\partial L}{\partial a_1} = \dfrac{2}{m-1}\displaystyle\sum_{i=0}^{n}\left(\dfrac{\sum_{j=i-\frac{m}{2}}^{j=i+\frac{m}{2}}\left(T_j^{m.sk} - T_j^{t.sk}\right)^2}{m-1} - \bar{v}\right) \\ \displaystyle\sum_{j=i-\frac{m}{2}}^{j=i+\frac{m}{2}}\left(T_j^{m.sk} - T_j^{t.sk}\right)t_j = 0 \\ \dots \\ \dfrac{\partial L}{\partial a_2} = \dfrac{2}{m-1}\displaystyle\sum_{i=0}^{n}\left(\dfrac{\sum_{j=i-\frac{m}{2}}^{j=i+\frac{m}{2}}\left(H_j - \left(T_j^{m.sk} - T_j^{t.sk}\right)\right)^2}{m-1} - \bar{v}\right) \\ \displaystyle\sum_{j=i-\frac{m}{2}}^{j=i+\frac{m}{2}}\left(T_j^{m.sk} - T_j^{t.sk}\right)t_j^2 = 0 \\ . \quad \dots \\ \dfrac{\partial L}{\partial a_n} = \dfrac{2}{m-1}\displaystyle\sum_{i=0}^{n}\left(\dfrac{\sum_{j=i-\frac{m}{2}}^{j=i+\frac{m}{2}}\left(T_j^{m.sk} - T_j^{t.sk}\right)^2}{m-1} - \bar{v}\right) \\ \displaystyle\sum_{j=i-\frac{m}{2}}^{j=i+\frac{m}{2}}\left(T_j^{m.sk} - T_j^{t.sk}\right)t_j^n = 0 \end{cases} \tag{6}$$

These equations can be solved using the theory of hypernumbers [12, 13] and derived from this theoretical method for solving operator equations [14]. This method has been applied to both thermal and stochastic processes [9–11].

The coefficient a_0 is defined from the best fit operator equation.

$$L_f = min \sum_{i=0}^{n}\left(T_i^{m.sk} - \left(a_0 + a_1 t_i + \dots + a_n t_i^n\right)\right)^2 \tag{7}$$

The solution of the (4) is defined with the theory of hypernumber.

$$H_k^{con} = a_0 + a_{1,k}t + a_{2,k}t^2 + \dots a_{n,k}t^n \tag{8}$$

Each consecutive hypernumber H_{k+1}^{con} is calculated from the previous one with the expression below:

$$H_{k+1}^{con} = H_k^{con} + \delta H_k^{con} \tag{9}$$

Where, δH_k^{con} is a deviation from the previous constructive number.

The deviation δH_n^{con} was computed by solving linear equations, and the convergence of the recursive algorithm was proven in [14].

The system of linear equations for δH_k^{con} sequential calculation is provided below.

$$\begin{cases} -\delta\left(\dfrac{\partial L}{\partial a_{1,k}}\right) \approx \dfrac{\partial^2 L}{\partial a_{1,k}^2}\delta a_{1,k} + \dfrac{\partial^2 L}{\partial a_{1,k}\partial a_{2,k}}\delta a_{2,k} + \cdots + \dfrac{\partial^2 L}{\partial a_{1,k}\partial a_{n,k}}\delta a_{n,k} = -\varepsilon\left(\dfrac{\partial L}{\partial a_{1,k}}\right) \\ -\delta\left(\dfrac{\partial L}{\partial a_{2,k}}\right) \approx \dfrac{\partial^2 L}{\partial a_{2,k}\partial a_{1,k}}\delta a_{1,k} + \dfrac{\partial^2 L}{\partial a_{2,k}^2}\delta a_{2,k} + \cdots + \dfrac{\partial^2 L}{\partial a_{2,k}\partial a_{n,k}}\delta a_{n,k} = -\varepsilon\left(\dfrac{\partial L}{\partial a_{2,k}}\right) \\ \cdots \\ -\delta\left(\dfrac{\partial L}{\partial a_{n,k}}\right) \approx \dfrac{\partial^2 L}{\partial a_{n,k}\partial a_{1,k}}\delta a_{1,k} + \dfrac{\partial^2 L}{\partial a_{n,k}\partial a_{2,k}}\delta a_{2,k} + \cdots + \dfrac{\partial^2 L}{\partial a_{n,k}^2}\delta a_{n,k} = -\varepsilon\left(\dfrac{\partial L}{\partial a_{n,k}}\right) \end{cases} \quad (10)$$

Per the defined H_k^{con}, the part of the condition of Equation (1) related to the skin temperature can be rewritten as

$$a_0 + a_{1,k}t + a_{2,k}t^2 + \ldots a_{n,k}t^n < t_{skin} \,\forall\, t \in [0, t_{mon} + t_{pred}] \quad (11)$$

As per research covered [21], a positive correlation exists between the slope of the skin temp changes and radiation intensity. Such correlation is illustrated in Figures 1, and 2 for RF radiation.

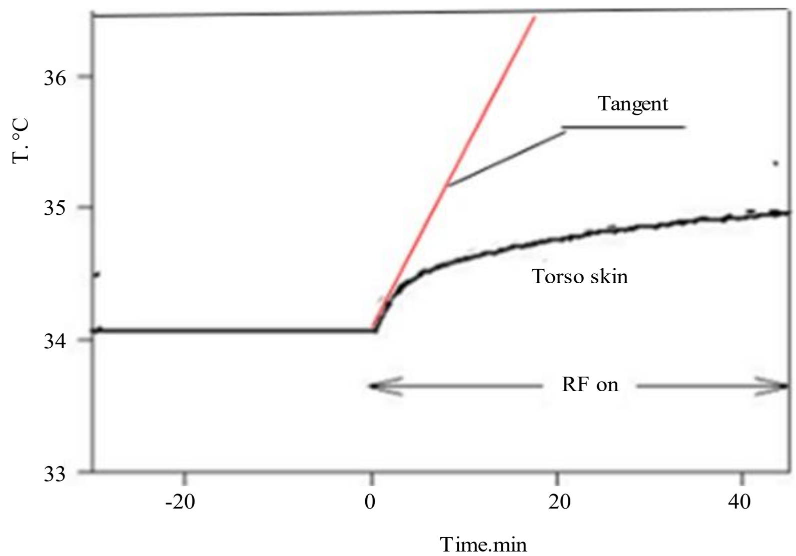

Figure 1. Changes in skin and core temperatures due to RF exposure at 240 W/m^2. The charts were constructed using the corresponding one from [21].

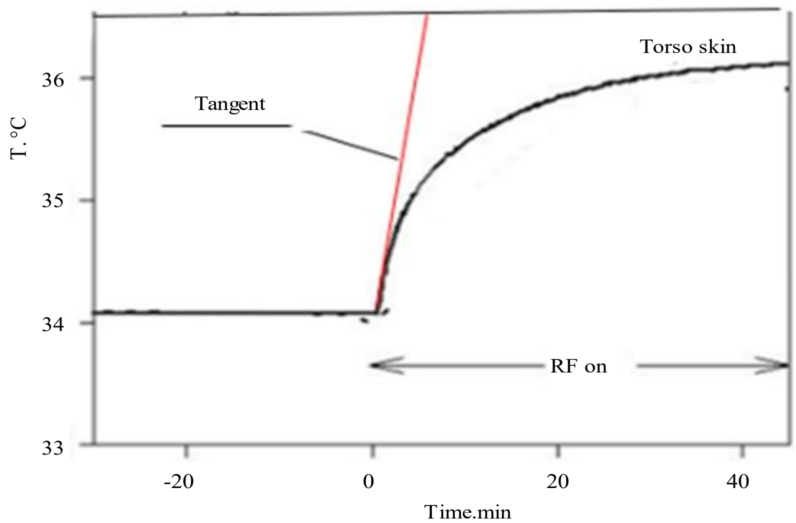

Figure 2. Changes in skin and core temperatures due to RF exposure at 350 W/m^2.

The charts were constructed using the corresponding one from [21].

Based on the assumption that a similar relationship exists between skin temperature changes and solar radiation intensity, the proposed expression is as follows:

$$\frac{\partial t_{skin}}{\partial t}(t_0) = F(q_r) \tag{12}$$

Skin Temperature Prediction

Equations 4-10 were used to predict the skin temperature. The results of the simulation with the Process Similarity Criteria Fit and minimum least-squares polynomials are shown in Figure 3.

The mean absolute percentage error (MAPE) error of the Best Criteria Fit was 0.235%, and the MAPE error of the minimum least square was 4,42%.

LSTM machine learning prediction was performed for the same training set to compare the RPPSCF efficiency. The simulation results are shown in Figure 4.

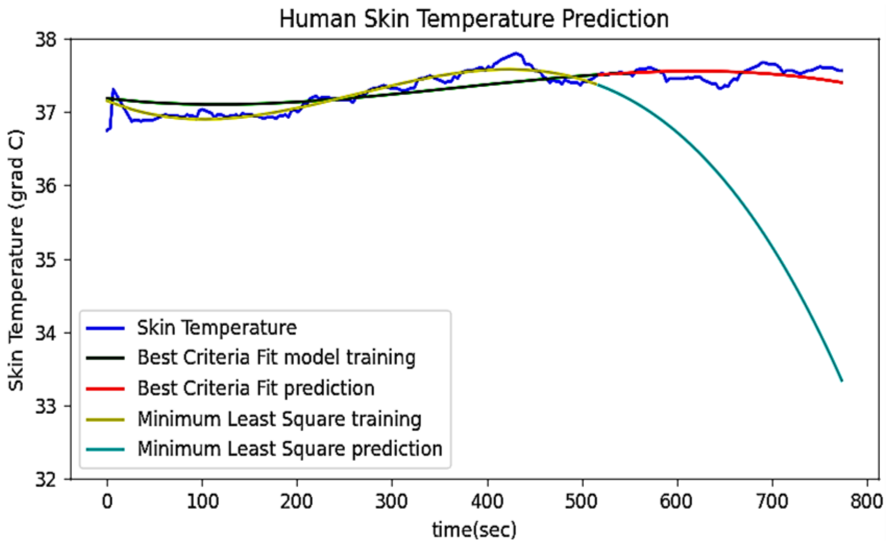

Figure 3. Human skin temperature prognostics using regression polynomial with similarity criteria and minimum least square. The data are retrieved from [22].

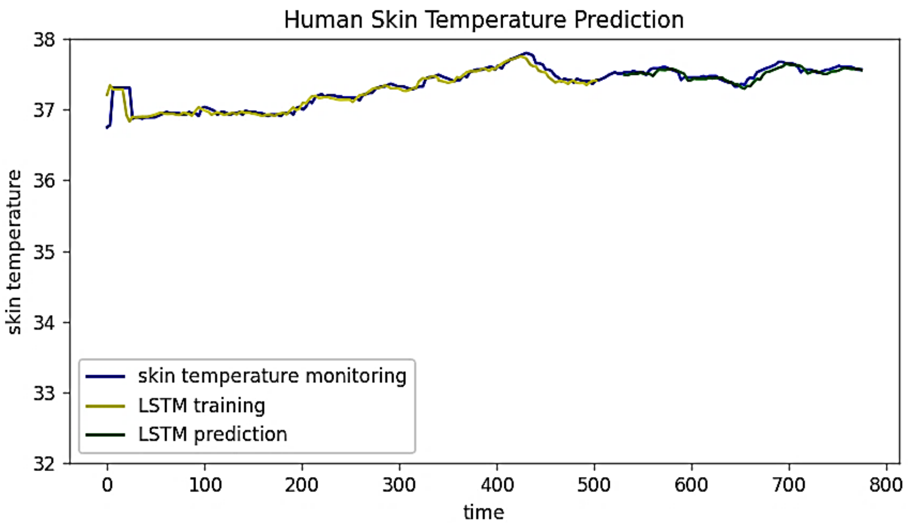

Figure 4. Human skin temperature prognostics using LSTM neural network. The MAPE error of LSTM was 0.0864%.

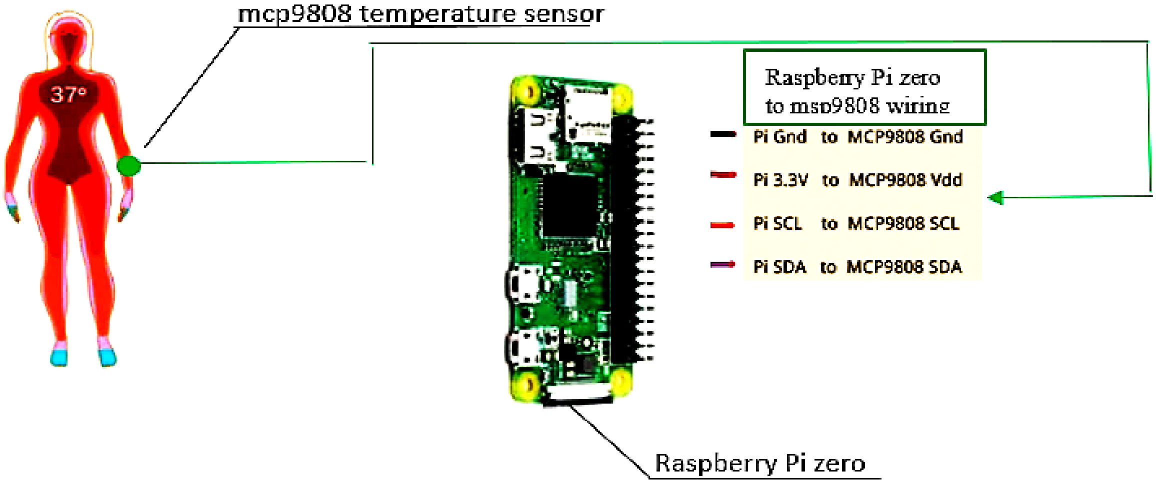

Figure 5. Schematic of skin temperature control.

Schema of the Skin Temperature Automated Control

Schematics of the skin temperature control and prediction are shown in Figure 5. The skin temperature was measured using an mcp9808 sensor. The sensor's accuracy is equals to 0.25°C. The DS18b20 sensor used for skin control in [23] has an accuracy of 0.5°C and is not suitable for good quality prediction. The alternative sensor tmp117 has an accuracy of 0.1°C. The schema and code for translating the data to the temperature were defined using Python for simulation [24, 25]. Raspberry PI Zero reads the sensor data. One of the possible results of delivery is sending it to mobile devices.

RESULTS AND DISCUSSION

The results of the prediction using the proposed model are summarized below.

- Model accuracy: 99.765%.
- Performance (time complexity**):** Execution time = 0.244 s.
- Applicability: The model is applicable for analyzing the effects of multiple factors on the skin.

The current limitation of the proposed prediction model is related to the fact that the function of radiation intensity is not defined. Therefore, the practical implementation of this method is limited to skin temperature predictions. However, the theoretical definition allows for an extension of the method for analyzing the radiation intensity.

CONCLUSION

The research covered in This paper presents a novel approach for predicting skin temperature. The advantages of this approach are as follows:

- This method provides an analytical expression for forecasting the skin temperature. It allows for the analysis of multiple factors of the impact of the sun's radiation on the human body.
- The accuracy of the RPPSCF was lower than that of the LSTM. However, the accuracy is high when this method is used for skin temperature prediction.
- The prototype device for temperature prediction comprises miniature low-cost electronic elements.
- The application of the algorithm can be extended to the analysis of human health parameters that require an analytical presentation and low computational complexity.

REFERENCES

1. Horton L, Brady J, Kincaid CM, Torres AE, Lim HW. The effects of infrared radiation on the human skin. Photodermatol Photoimmunol Photomed. 2023;39:549–55. DOI: 10.1111/phpp.12899, PubMed: 37431693.

2. Marion JW, Lee J, Rosenblum JS, Buckley TJ. Assessment of temperature and ultraviolet radiation effects on sunburn incidence at an inland U.S. beach: A cohort study. Environ Res. 2018;161:479–84. DOI: 10.1016/j.envres.2017.11.036, PubMed: 29220801.
3. Kricker A, Armstrong BK, Goumas C, Litchfield M, Begg CB, Hummer AJ, et al. Ambient UV, personal sun exposure and risk of multiple primary melanomas. Cancer Causes Control. 2007;18:295–304. DOI: 10.1007/s10552-006-0091-x, PubMed: 17206532.
4. Petersen B, Philipsen PA, Wulf HC. Skin temperature during sunbathing—Relevance for skin cancer. Photochem Photobiol Sci. 2014;13:1123–5. DOI: 10.1039/c4pp00066h, PubMed: 24930491.
5. Moore HM, Bai B, Boisvert FM, Latonen L, Rantanen V, Simpson JC, et al. Quantitative proteomics and dynamic imaging of the nucleolus reveal distinct responses to UV and ionizing radiation. Mol Cell Proteomics. 2011;10.009241. DOI: 10.1074/mcp.M111.009241, PubMed: 21778410.
6. Cho S, Shin MH, Kim YK, Seo JE, Lee YM, Park CH, et al. Effects of infrared radiation and heat on human skin aging in vivo. J Invest Dermatol Symp Proc. 2009;14:15–9. DOI: 10.1038/jidsymp.2009.7, PubMed: 19675547.
7. Finlayson L, Barnard IRM, McMillan L, Ibbotson SH, Brown CTA, Eadie E, et al. Depth penetration of light into skin as a function of wavelength from 200 to 1000 nm. Photochem Photobiol. 2022;98:974–81. DOI: 10.1111/php.13550, PubMed: 34699624.
8. Ash C, Dubec M, Donne K, Bashford T. Effect of wavelength and beam width on penetration in light-tissue interaction using computational methods. Lasers Med Sci. 2017;32:1909–18. DOI: 10.1007/s10103-017-2317-4, PubMed: 28900751.
9. Burgin M, Dantsker AM. Real-time inverse modeling of control systems using hypernumbers. In: Functional Analysis and Probability. New York: Nova Science Publishers; 2015. p. 439–56.
10. Burgin M. Semitopological vector spaces: Hypernorms, hyperseminorms, and operators. Oakville: Apple Academic Press; 2017.
11. Dantsker A, Burgin M. Monitoring thermal conditions and finding sources of overheating. In: Proceedings of the 2021 Summit of the International Society for the Study of Information. 2022. DOI: 10.3390/proceedings2022081038.
12. Burgin M. Hypernumbers and extrafunctions: Extending the classical calculus. New York: Springer Science+Business Media; 2012.
13. Burgin M. Integration in bundles with a hyperspace base: Indefinite integration. In: Topics in Integration Research. New York: Nova Science Publishers; 2013.
14. Burgin M, Dantzler A. A method of solving operator equations of mechanics with the theory of hypernumbers. Notices Natl Acad Sci Ukraine. 1995;8:27–30.
15. Lai D, Zhou X, Chen Q. Measurements and predictions of the skin temperature of human subjects on outdoor environments. Energy Build. 2017;151:476–86. DOI: 10.1016/j.enbuild.2017.07.009.
16. Zhou W, Yang M, Yu X, Peng Y, Fan C, Xu D, et al. Enhancing thermal comfort prediction in high-speed trains through machine learning and physiological signals integration. J Therm Biol. 2024;121:103828. DOI: 10.1016/j.jtherbio.2024.103828, PubMed: 38604115.
17. Cheng X, Yang B, Tan K, Isaksson E, Li L, Hedman A, et al. Non-invasive measuring method of skin temperature based on skin sensitivity index and deep learning. [pre-print]. 2018;arXiv:1812.06509. DOI: 10.48550/arXiv.1812.06509.
18. Gorczyca MT, Milan HFM, Maia ASC, Gebremedhin KG. Machine learning algorithms to predict core, skin, and hair-coat temperatures of piglets. Comput Electron Agric. 2018;151:286–94. DOI: 10.1016/j.compag.2018.06.028.
19. Dantsker A, Brito J, Pryor W. Defining regression polynomials with process similarity criteria. Res Rev. 2023;10.
20. Keogh E, Chu S, Hart D, Pazzani M. A survey and novel approach. Segmenting time series. Ser Mach Percept Artif Intell. 2004;1–21.
21. Foster KR, Adair ER. Modeling thermal responses in human subjects following extended exposure to radiofrequency energy. Biomed Eng Online. 2004;3:4. DOI: 10.1186/1475-925X-3-4, PubMed: 14989757.

22. Kurazumi Y, Fukagawa K, Sakoi T, Aruninta A, Kondo E, Yamashita K. Skin temperature and body surface section in non-uniform and asymmetric outdoor thermal environment. Health. 2018;10:1321–41. DOI: 10.4236/health.2018.1010102.
23. Sollu TS, Alamsyah, Bachtiar M, Bontong B. Monitoring system heartbeat and body temperature using Raspberry Pi. E3S Web Conf. 2018;73:12003. DOI: 10.1051/e3sconf/20187312003.
24. Siepert B. (2020). Adafruit TMP117 High Accuracy I2C Temperature Monitor. [online] Adafruit Learning System. Available from: https://learn.adafruit.com/adafruit-tmp117-high-accuracy-i2c-temperature-monitor/overview
25. DiCola T. (2014). MCP9808 Temperature Sensor Python Library. [online] Adafruit Learning System. Available from: https://learn.adafruit.com/mcp9808-temperature-sensor-python-library/overview

